



CELLULAR AND MOLECULAR BIOLOGY

Patterns of genetic diversity, spatial genetic structure and gene flow in *Campomanesia xanthocarpa*: insights from SSR markers of different genomic origins

VANESSA S. PETRY, VALDIR M. STEFENON, LILIAN O. MACHADO, NEWTON C.F. DA COSTA, GUSTAVO H.F. KLABUNDE & RUBENS O. NODARI

Abstract: *Campomanesia xanthocarpa* (Mart.) O. Berg is a South American fruit tree species with important ecological and medicinal properties, which remnants are currently found mainly in isolated forest fragments. In this study, SSR markers from three different genomic origins (gene-linked, nuclear neutral, and organellar) were used to evaluate the patterns of genetic diversity, fine-scale spatial genetic structure and historical gene flow in fragmented forest formations of *C. xanthocarpa* from the Atlantic Forest in southern Brazil. Our results show that the forest fragments present moderate to high levels of genetic diversity in comparison to species presenting similar life traits, although a trend opposite to expected was observed concerning gene-linked and neutral SSR markers. The fine-scale spatial genetic structure revealed different patterns in short and large distance classes, with a distinct influence of gene-linked and neutral markers in driving the genetic structure in each distance class. The presence of an isolation-by-adaptation pattern implies the need for maintenance of the current remnants to assure the conservation of the private alleles. Finally, as the genetic diversity is found predominantly within forest fragments, programs of seed collection and/or genetic rescue should prioritize a larger number of individuals within each fragment, to increase the sampled diversity.

Key words: Genetic structure, guabirola, isolation by distance, isolation by environment, microsatellite markers.

INTRODUCTION

More than a third of the world's forest cover was lost as a result of deforestation, which was widespread in temperate regions in the mid-18th to 20th centuries and increased in the tropics over the past half-century (Haddad et al. 2015). Consequently, remnant forests are likely to suffer from being smaller, more isolated, and with a greater area located near the edge of the forest (Haddad et al. 2015). In addition to the edge effect, fragmentation triggers the spatial distribution of plants to change and may also

affect the abundance and foraging behavior of pollinators (Breed et al. 2015). Such processes, in turn, may have negative ecological and genetic consequences in tree populations.

Habitat fragmentation and pollinators' decline are expected to impact the capacity of plant populations to reproduce successfully, generating concerns for their demography, evolution, and long-term persistence. Therefore, understanding the biology of plant reproduction is of central importance for dealing with these environmental challenges and for maintaining

biodiversity, genetic resources, and human well-being (Stefenon et al. 2020).

Breed et al. (2015) performed a comprehensive study aiming to test whether human-mediated forest fragmentation is correlated with changes in selfing rates, biparental inbreeding, and correlated paternity. This study advocated that the negative effect of habitat fragmentation on mating patterns is a general trend for animal-pollinated woody plants. However, fragment boundaries may not represent restrictions for mating populations of trees that benefit from long-distance pollination and/or long-distance seed dispersal (Kramer et al. 2008). Moreover, the consequences of fragmentation may have quite distinct effects in different species (Kramer et al. 2008). While the genetic diversity decreased in *Araucaria angustifolia* (Auler et al. 2002) and *Cariniana legalis* (Tambarussi et al. 2016), genetic diversity was not affected by forest fragmentation in species as *Sorocia bonplani* (Ruschel et al. 2007) and *Cercis canadensis* (Orni et al. 2020).

Campomanesia xanthocarpa (Mart.) O. Berg (Myrtaceae) is a fruit tree species native to the Brazilian Atlantic Forest, also occurring in Argentina, Uruguay, and Paraguay (Legrand & Klein 1977). The fruits of *C. xanthocarpa* are small (2-3 cm long) and berry-type, globose with a yellowish, smooth, and thin epicarp when ripe, containing a juicy pulp with an aromatic and pleasant flavor. These fruits are an important feed source for the local fauna, while their major economic uses are domestic consumption and small-scale marketing by small farmers (Lisbôa et al. 2011) and also indicated as a functional food (Viecili et al. 2014). Several medicinal properties have been recently reported for this species (de Paulo Farias et al. 2020), although native people have been using it for a long time ago. Among the therapeutic properties of leaves and fruits of *C. xanthocarpa* are the antidiarrheal

(Souza-Moreira et al. 2011), antioxidant (Pereira et al. 2012), and trypanocidal (Salmazzo et al. 2019) purposes. This species was also found to exhibit therapeutic properties in metabolic disorders (Cardozo et al. 2018), in dyslipidemias prevention (Sousa et al. 2019), as well as photoprotective potential (Catelan et al. 2019), and antitumoral function (Amaral et al. 2019).

As an effect of the advances of agriculture and logging for timber over the last three centuries (Haddad et al. 2015), the once contiguous forest formations of the Brazilian Atlantic Forest currently form a largely deforested landscape. Most of the forest remnants in the Brazilian Atlantic Forest are formed for small fragments within 100 m of an edge (Haddad et al. 2015, Santos et al. 2019). Consequently, native tree species of this biome are found as small and relatively isolated forest formations laying within an anthropized matrix of urban and agricultural lands (Brocardo et al. 2018, Palmeirim et al. 2019, Lautejung et al. 2019).

The central aim of our study was to use SSR (microsatellite) markers from three different genomic origins to evaluate the patterns of genetic diversity, fine-scale spatial genetic structure, and historical gene flow in fragmented forest formations of *C. xanthocarpa* in southern Brazil. Microsatellite markers found within expressed regions of the nuclear genome (gene-linked markers) are interconnected to genomic regions which may be under selection pressure and may express measurements of selective DNA variation. On the other hand, microsatellite loci located in non-expressed regions of the nuclear genome are considered selectively neutral markers, measuring neutral DNA variation (although some can be in linkage disequilibrium with selected regions). Organellar microsatellite markers, in turn, can be found in the mitochondrial or the plastid genomes and are very useful for phylogenetic, phylogeographic,

and population genetic studies, mainly because of the predominantly uniparental heritability and the absence of recombination (Lemos et al. 2018). Employing neutral, gene-linked, and organellar SSR markers, we intended to assess the evolutive history of a forest tree species with geographically fragmented distribution in the subtropical region of the Brazilian Atlantic Forest. In addition, we evaluated the impact of the genomic origin of the markers in accessing and estimating such genetic diversity parameters. Using this approach, four main hypotheses were tested: (1) as an effect of the deforestation and consequent fragments disconnection, the historical gene flow within and among forest fragments of *C. xanthocarpa* follow an isolation-by-distance pattern; (2) the reduced size of the forest fragments decreases the number of pollen and seed dispersers, generating a high fine-scale spatial genetic structure; (3) given the haploid nature and absence of recombination of the mitochondrial and plastid genomes, organellar markers present lower genetic diversity within fragment and higher differentiation among fragments, in comparison to nuclear markers; and (4) since expressed regions of the genome are more conserved, neutral nuclear SSR markers will reveal higher differentiation both within and among forest fragments in comparison to gene-linked SSRs.

MATERIALS AND METHODS

Sample collection and genotyping

A total of 200 adult plants of *C. xanthocarpa* were sampled in four forest fragments located in southern Brazil (Figure 1a-f): Coronel Freitas (26°48'33"S, 52°42'22"W; hereafter called CF), Iomerê (27°00'26"S, 51°14'28"W; hereafter called IOM), São Joaquim (28°28'38"S, 50°04'04"W; hereafter called SJ) and São José do Cerrito (27°43'30"S, 50°36'21"W; hereafter called SJC).

We collected 50 adult trees in each sampling site keeping a distance from 15 to 20 m among plants within each fragment (Figure 1c-f). Fragments CF (Figure 1c), IOM (Figure 1e), and SJC (Figure 1f) are ranching areas with some trees growing within riparian forests and some trees located within grassland zones. All adult trees in fragment SJC were sampled. Fragment SJ (Figure 1d) is a remnant of a riparian forest at Pelotas river. This area lacks current management, but experienced fragmentation during the period of wood exploitation in Southern Brazil, in the 1960-1970s. All sampled trees were georeferenced using a navigation GPS Garmin MAP 60 CSX. Voucher specimens from each forest fragment were deposited in the herbaria FLOR (Department of Botany of the Federal University of Santa Catarina, Florianópolis, SC, Brazil; vouchers FLOR 63645 and FLOR 63646 consigned forest fragments Coronel Freitas and Iomerê, respectively), and LUSC (the University of the State of Santa Catarina, Lages, SC, Brazil; vouchers LUSC 8707 and LUSC 7870 consigned forest fragments São Joaquim and São José do Cerrito, respectively). Total DNA was extracted from leaves dried in silica gel, using the CTAB method (Doyle & Doyle 1990).

Four neutral nuclear, two gene-linked, and three organellar SSR markers described by Petry et al. (2019) were employed in this study. PCR amplifications were performed individually or in multiplex reactions (Petry et al. 2019). Loci Cxant50, Cxant66, Cxant69, and Cxant76 were individually amplified in 20 µL reactions containing 20 ng of DNA, 0.2 mM of each dNTP (Invitrogen, Carlsbad, CA, USA), 1 U of Taq DNA polymerase (QuatroG, Porto Alegre, RS, Brazil), 1X buffer, 1.5 mM of MgCl₂ and 0.2 µM of each primer. Amplifications were performed in a Veriti™ Thermal Cycler (Applied Biosystems, Foster City, CA, USA) with an initial denaturing step at 95 °C for 3 min, followed by 30 cycles

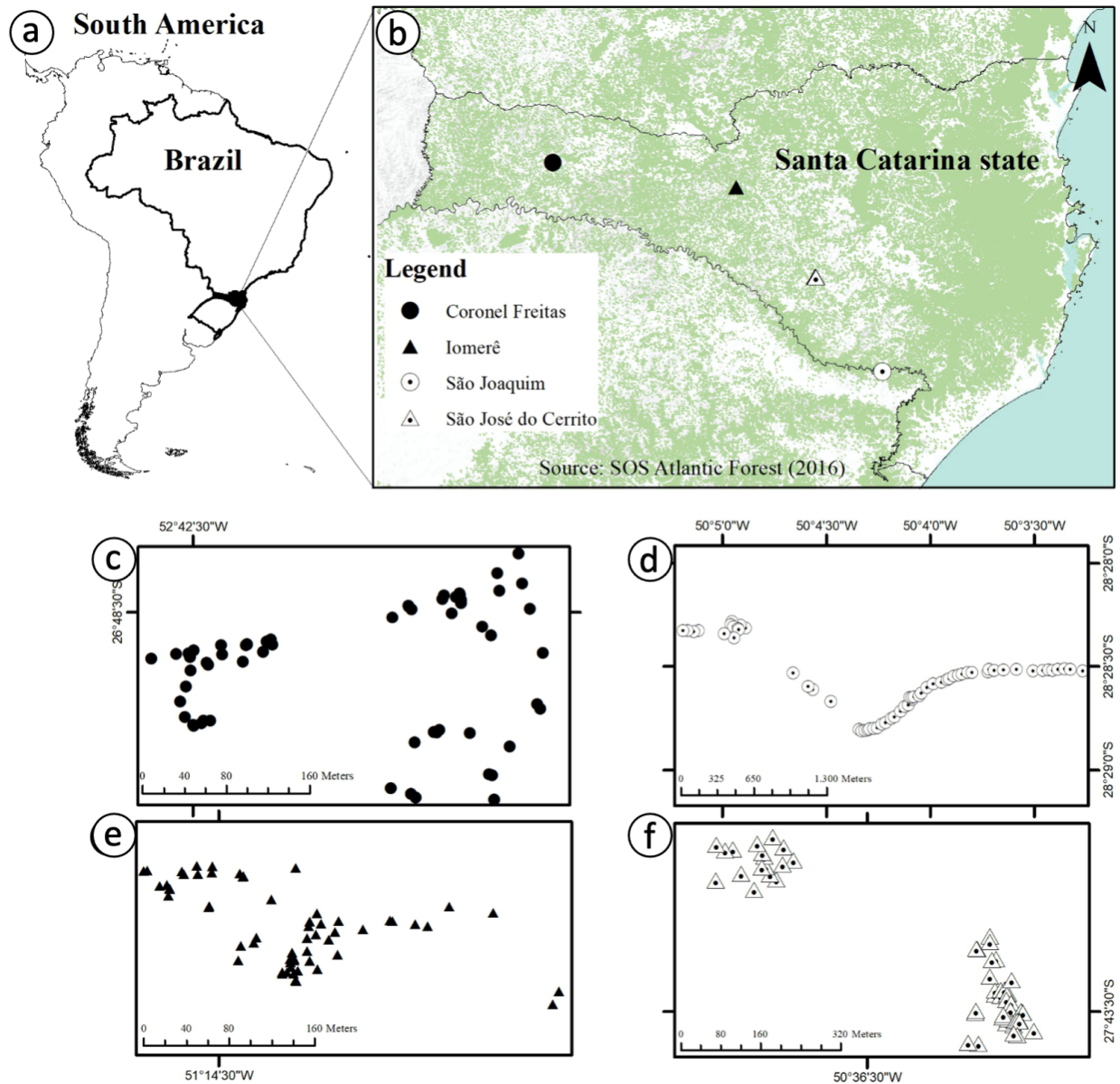


Figure 1. Geographic location of the forest fragments of *C. xanthocarpa* evaluated in this study. (a) Location of the Santa Catarina State in Southern Brazil. (b) Distribution of the forest fragments within Santa Catarina State. (c-f) Geographic distribution of sampled plants within each forest fragment: (c) Coronel Freitas, (d) São Joaquim, (e) Iomerê, and (f) São José do Cerrito.

of 94 °C for 30 s, annealing temperature (66 °C for Cxant50, 57 °C for Cxant66, 60 °C for Cxant69 and Cxant76) for 30 s and extension at 72 °C for 1 min, with a final extension step of 72 °C for 30 min. The other five loci were combined in biplex (Cxant59/Gauabi05) or triplex (Cxant22/Cxant26/Gauabi11) in a reaction volume of 6.2

μL reaction mix, containing 12 ng of DNA, 2.1 μL of QIAGEN Multiplex PCR Master Mix (Qiagen Inc., Valencia, CA, USA) and 0.10-0.40 μM of each primer (see Petry et al. 2019). Amplifications were carried out in a Veriti™ Thermal Cycler with an initial denaturing step at 95 °C for 15 min, followed by 25 cycles of 94 °C for 30 s, annealing

temperature (55 °C for Cxant59 and Guabi05, or 57 °C for Cxant22, Cxant26, and Guabi11) for 30 s and extension at 72 °C for 1 min, with a final extension step of 60 °C for 30 min. To all nine loci, the forward primers were 5' labeled with fluorescent dyes (PET, 6-FAM, NED, or VIC).

Amplified alleles were resolved through capillary electrophoresis using an ABI 3500xL DNA automatic sequencer (Applied Biosystems), with the POP-7™ polymer (Applied Biosystems). The reactions were adjusted to a final volume of 11 µL, including 1 µL of PCR product, 0.3 µL of GeneScan 600 Liz genotyping size standard (Applied Biosystems), and 9.7 µL Hi-Di™ formamide (Applied Biosystems). Allele calling was carried out with previously defined bins using the software GeneMapper® version 3.2 (Applied Biosystems).

Estimates of genetic diversity within forest fragments

The software GenAEx version 6.5 (Peakall & Smouse 2012) was employed to estimate the total number of alleles (A), the effective number of alleles (A_e), unbiased expected heterozygosity (H_e), and the fixation indexes at forest fragment (F) and mean population (F_{IS}) levels for nuclear loci (neutral and gene-linked), and the total number of alleles (A), the effective number of alleles (A_e), and haploid gene diversity (h) for the organellar markers. The statistical significance of the F_{IS} estimates was determined through the Fisher's exact test using a Markov Chain method (1000 dememorization steps, 100 batches, and 1000 iterations per batch), as performed in the GenePop on web version 4.6 (<http://genepop.curtin.edu.au>) (Rousset 2008). Significant evidence of null alleles was identified in loci Cxant50 and Cxant76, but no evidence of putative physical linkage between pairs of loci was verified for these markers (Petry et al. 2019).

Analysis of the fine-scale spatial genetic structure

Fine-scale spatial genetic structure (SGS) within each forest fragment was estimated using the nuclear markers at three different levels: all nuclear markers, neutral markers, and gene-linked markers. The pairwise correlation between plants within each distance interval was computed using the kinship coefficients (F_{ij}), according to Loiselle et al. (1995). The number of distance classes (distance intervals within which the pairs of plants are considered) was determined for each forest fragment so that an even number of pairs of individuals was analyzed across distance classes. The statistical significance of F_{ij} was determined after 10,000 permutations of alleles among individuals.

The relationship of genetic similarity and geographic distance between individuals was computed for each forest fragment as the regression slope of the F_{ij} kinship coefficient (b_F) on the distance. To quantify the SGS and quantitatively compare it among forest fragments, we computed the S_p statistic (Vekemans & Hardy 2004) for each forest fragment, based on the regression slope of kinship coefficients, as $S_p = -b_F / (1 - F_1)$, where F_1 is the mean kinship coefficient between individuals belonging to the first distance class. All estimates of fine-scale spatial genetic structure were performed using the software Spagedi 1.2 (Hardy & Vekemans 2002).

Analysis of genetic structure and differentiation among forest fragments

Overall and pairwise population variations were evaluated based on estimations of G_{ST} corrected for small number of populations (Meirmans & Hendrix 2011) and Jost's D , using the software GenAEx version 6.5 (Peakall & Smouse 2012), at three levels: all nuclear markers, neutral markers, and gene-linked markers. The G_{ST} estimation

quantifies nearness to fixation and estimates values of demographic parameters. The Jost's D estimate quantifies the relative degree of allelic differentiation (Jost et al. 2017).

Additionally, the genetic structure at forest fragment level was estimated by plotting the pairwise genetic differentiation estimated as $F_{ST} / (1 - F_{ST})$, against the geographic distance between forest fragment pairs. The analysis was performed at three different levels (all nuclear markers, neutral markers, and gene-linked markers), as for the fine-scale spatial genetic structure. The analysis was achieved in the software Spagedi 1.2 (Hardy & Vekemans 2002). Statistical significance of the genetic differentiation was determined after 10,000 permutations of alleles among individuals.

Both non-hierarchical analyses of molecular variance (AMOVA) and multivariate analysis (PCO) were utilized to evaluate the genetic differentiation among forest fragments. These two analyses were performed using GenAlEx version 6.5, at four levels: organellar markers, all nuclear markers, neutral markers, and gene-linked markers.

Estimation of the pairwise historical gene flow

Historical gene flow among forest fragments was estimated as the number of migrants between fragment pairs using a coalescent-based model with a Bayesian inference approach, as implemented in the software Migrate-n (Beerli 2016). Computations were performed through the online platform **CIPRES Science Gateway V. 3.3** (<https://www.phylo.org>). The number of migrants per generation was determined as $Nm_{i \rightarrow j} = M_{i \rightarrow j} \times \theta_j$ (Beerli & Felsenstein 1999), where $M_{i \rightarrow j} = m / \theta \times \mu$ is the scaled immigration rate from forest fragment i into forest fragment j and $\theta_j = 4 \times N_e \times \mu$ is the effective size of the recipient forest fragment conditional on the underlying genealogy. The unknown mutation

rate (μ) is absorbed into the parameters θ and M , which are initially generated from F_{ST} -calculations. Computations were executed under a constant mutation rate for all loci, using a Brownian motion mutation model. The Markov Chain Monte Carlo (MCMC) simulations were run in triplicate using three long chains (increment = 100; genealogies sampled = 100,000, genealogies recorded per chain = 5000; burn-in = 10,000). An adaptive "heating scheme" was used to search for additional compatible genealogies using four chains with four temperatures: 1.0, 1.5, 3.0, and 100,000. Results were obtained as the mean of the three runs. The robustness of the estimated parameters was determined through the convergence of the MCMC, evaluated through the effective sample size (ESS). $ESS > 200$ assures that the MCMC simulation provided a confident estimate of the parameters' posterior distribution.

Analysis of nuclear loci potentially under selection

In order to evaluate the occurrence of natural selection over the nuclear microsatellite loci, the approach of Beaumont & Nichols (1996) was employed. This analysis is based on plotting the F_{ST} distribution of each locus as a function of the heterozygosity. Allele frequencies estimations and coalescent simulations are used to generate a null sampling distribution of F_{ST} estimations based upon neutrality. Loci potentially under selection are expected to present an F_{ST} estimation significantly higher than expected under neutrality, being plotted outside the 95% confidence interval of the null distribution. The 5% and 95% limits of the null distribution were determined through 10,000 simulations of the coalescence process. All estimations were achieved in the Arlequin 3.5 software (Excoffier et al. 2005).

RESULTS

Levels of genetic diversity within each forest fragment

The estimates of genetic diversity (A , A_e , H_e , and h) revealed singular patterns for each class of genetic marker evaluated (Table I). As expected, higher estimations of A and A_e ($p < 0.05$ in fragment IOM and $p > 0.05$ for all other

fragments) were revealed for nuclear markers in comparison to organellar ones. However, higher estimates were also observed for the gene-linked markers, in comparison to neutral nuclear markers for A , A_e ($p < 0.05$ in fragment CF and $p > 0.05$ for all other fragments) and H_e ($p < 0.05$ in fragments CF and IOM and $p > 0.05$ for all other fragments), but not for the fixation indexes F_{IS} and F_{IT} . When estimates were obtained for all

Table I. Genetic diversity indices at forest fragment level and overall fragments, for each microsatellite marker class.

Marker	Forest fragment	Genetic diversity indices				
		A	A_e	H_e	H_o	F_{IS}
Neutral markers	CF	2.75	1.67 ^a	0.40 ^a	0.35	0.15 ^{***}
	IOM	2.50	1.61	0.38 ^b	0.34	0.08 ^{ns}
	SJ	2.75	1.97	0.42	0.30	0.14 ^{ns}
	SJC	3.00	1.94	0.48	0.43	0.06 ^{***}
	Overall	2.75	1.79	0.42	0.36	0.12 ^{***}
Gene-linked markers	CF	5.50	2.93 ^a	0.67 ^a	0.48	0.27 ^{ns}
	IOM	4.50	2.18	0.54 ^b	0.41	0.21 ^{ns}
	SJ	3.00	1.70	0.40	0.50	-0.11 ^{***}
	SJC	4.00	2.27	0.56	0.60	-0.11 ^{ns}
	Overall	3.25	1.96	0.46	0.50	0.10 ^{ns}
All nuclear markers	CF	3.67	2.09	0.49	0.39	0.19 ^{***}
	IOM	3.17 ^c	1.80 ^c	0.43	0.36	0.12 ^{ns}
	SJ	2.83	1.88	0.41	0.37	0.06 ^{ns}
	SJC	3.33	2.05	0.50	0.48	0.001 ^{**}
	Overall	4.25	2.27	0.54	0.40	0.08 ^{ns}
		A	A_e	h	-	-
Organellar markers	CF	2.33	2.01	0.51	-	-
	IOM	1.33 ^c	1.07 ^c	0.06	-	-
	SJ	2.00	1.35	0.17	-	-
	SJC	2.67	1.49	0.29	-	-
	Overall	2.08	1.48	0.26	-	-

^a estimations of A_e and H_e are significantly different ($p < 0.05$) between neutral and gene-linked markers for forest fragment CF according to a t-test.

^b estimations of H_e are significantly different ($p < 0.05$) between neutral and gene-linked markers for forest fragment IOM according to a t-test.

^c estimations of A and A_e are significantly different ($p < 0.05$) between nuclear and organellar markers for forest fragment IOM according to a t-test.

Statistical significance of the F_{IS} values: *** = $p < 0.001$; ** = $p < 0.01$; ns = not significant

nuclear markers together, values of A , A_e and H_e were higher, and values of overall F_{IS} and F_{IT} were lower than those obtained for gene-linked ($F_{IS} = 0.10$ versus $F_{IT} = 0.14$) and neutral markers alone ($F_{IS} = 0.12$ versus $F_{IT} = 0.17$). Population SJC presented the highest estimations of H_e for nuclear markers (for all three levels), while CF fragment presented the highest estimation of h for organellar markers.

Patterns of fine-scale spatial genetic structure

The patterns of spatial genetic structure within forest fragments were assessed only using the nuclear markers at three levels. Despite the small number of markers used (four neutral and two gene-linked markers), this approach allowed us to guess which marker category (gene-linked or neutral marker) presented the highest influence at the shortest and the largest distances classes, by comparing their slope patterns with the analysis obtained with all nuclear markers together.

CF fragment showed a comparatively high kinship coefficient value ($F_{ij} = 0.0319$) in the first

distance class for the analysis using all nuclear markers (Figure 2), suggesting the presence of family-structure. However, the overall slope of the analysis does not support a pattern of isolation by distance (IBD), in which the pairwise kinship of the pairs of trees declines with the increase of the distance. In this forest fragment, the gene-linked markers determined the slope pattern of the three shortest distance classes, while neutral markers were dominant in determining the pattern observed in the three largest distance classes.

No significant deviation of the random spatial distribution of genotypes was verified in fragment IOM for all three analyses. However, it is clear that gene-linked markers shape the slope pattern of the shortest distance classes, while neutral markers determine the largest distance classes. In these forest fragments too, no pattern of IBD is observed. Neutral markers were the main responsible for the slope pattern of both the shortest and largest distance classes in the SJ fragment. However, at an intermediate distance class (1973 m), gene-linked markers

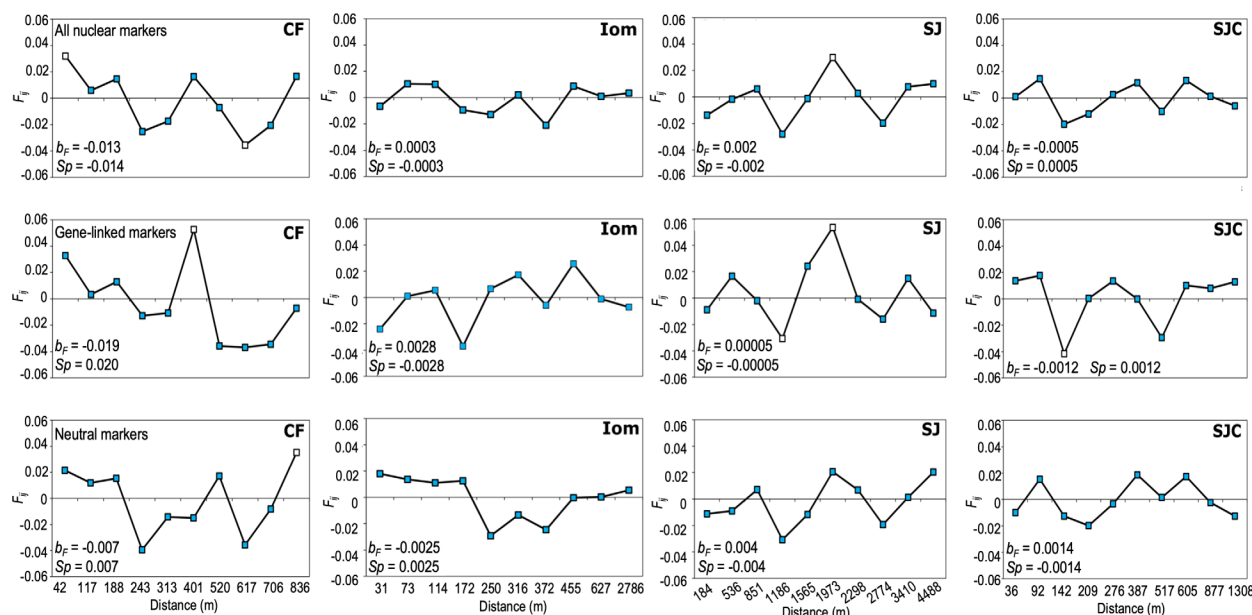


Figure 2. Correlograms of kinship coefficient measures (F_{ij}) plotted against the distance between trees of forest fragments of *C. xanthocarpa*. Not filled squares are significant at the 5 % level.

caused high influence, perceived in a significantly high estimation of F_{ij} . SJC fragment presented no values of F_{ij} outside the 95% probability envelop and, similarly to SJ fragment, has the neutral markers shaping its spatial genetic structure pattern. Based on the estimations of S_p -statistics, all forest fragments exhibited a low level of spatial genetic structure. Although low, the CF fragment revealed the highest level of S_p (0.014) among the four evaluated forest fragments.

Genetic structure and differentiation among forest fragments

Overall differentiation based on G_{ST} was higher than the estimations based on Jost's D for all nuclear markers ($G_{ST} = 0.146$ vs $D = 0.073$), gene-linked markers ($G_{ST} = 0.177$ vs $D = 0.105$), and neutral markers ($G_{ST} = 0.134$ vs $D = 0.061$). The same pattern was observed for the pairwise estimations of G_{ST} and D (Table III).

The pairwise estimations of spatial genetic structure between fragments refuted a pattern of IBD in all levels of analysis (all nuclear, gene-linked, and neutral markers, Figure 3). Similarly, the AMOVA analysis of the nuclear markers demonstrated a low level of differentiation among forest fragments (6%-7%) and 93%-94% of differentiation within forest fragments (Table II). Organellar markers revealed 81% of differentiation within forest fragments and 19% among forest fragments, suggesting lower organellar gene flow in comparison to nuclear markers.

The ordination analysis (PCoA, Figure 4) revealed higher genetic similarity between IOM and CF forest fragments (mainly for gene-linked and all nuclear markers). Also, in this analysis, the distance between forest fragments did not determine genetic distinctness.

Scaled effective sizes and pairwise gene flow

The estimations of the scaled effective size of the forest fragments and pairwise gene flow presented highly confident results, with effective sample size values higher than 153475.5 (Table III). All forest fragments revealed similar estimations of the effective size ($\theta \sim 0.09$). The number of migrants per generation ranged from 3.18 from SJ fragment into CF fragment ($Nm_{SJ \rightarrow CF}$), to 56.43 from SJC fragment into CF fragment ($Nm_{SJC \rightarrow CF}$). Out of the 12 estimations of pairwise gene flow, four presented values higher than the 97.5% percentile ($Nm_{IOM \rightarrow CF}$, $Nm_{CF \rightarrow SJ}$, $Nm_{IOM \rightarrow SJC}$, $Nm_{SJ \rightarrow SJC}$) suggesting a gene flow higher than expected only by chance. There was no significant correlation (Spearman $r_s = 0.13$, $p = 0.70$) between geographic distance and gene flow. The number of migrants from SJ into SJC is five-fold higher than in the opposite direction (i.e., from SJC into SJ), four-fold higher from CF into SJ than from SJ into CF, and two-fold higher from IOM into SJC than in the opposite direction.

SSR loci potentially under selection

Despite the influence of gene-linked markers in shaping the pattern of spatial genetic structure in CF and IOM forest fragments (Figure 2), none of the loci presented a behavior deviating from neutrality (Figure 5). Only locus Cxant26 presented an F_{ST} estimation slightly below the 0.05 limit of the significance interval. However, this small deviation should not be considered evidence of selection under this locus since the analysis search for loci with F_{ST} values significantly above the 95% limit, meaning high differentiation among fragments at such markers.

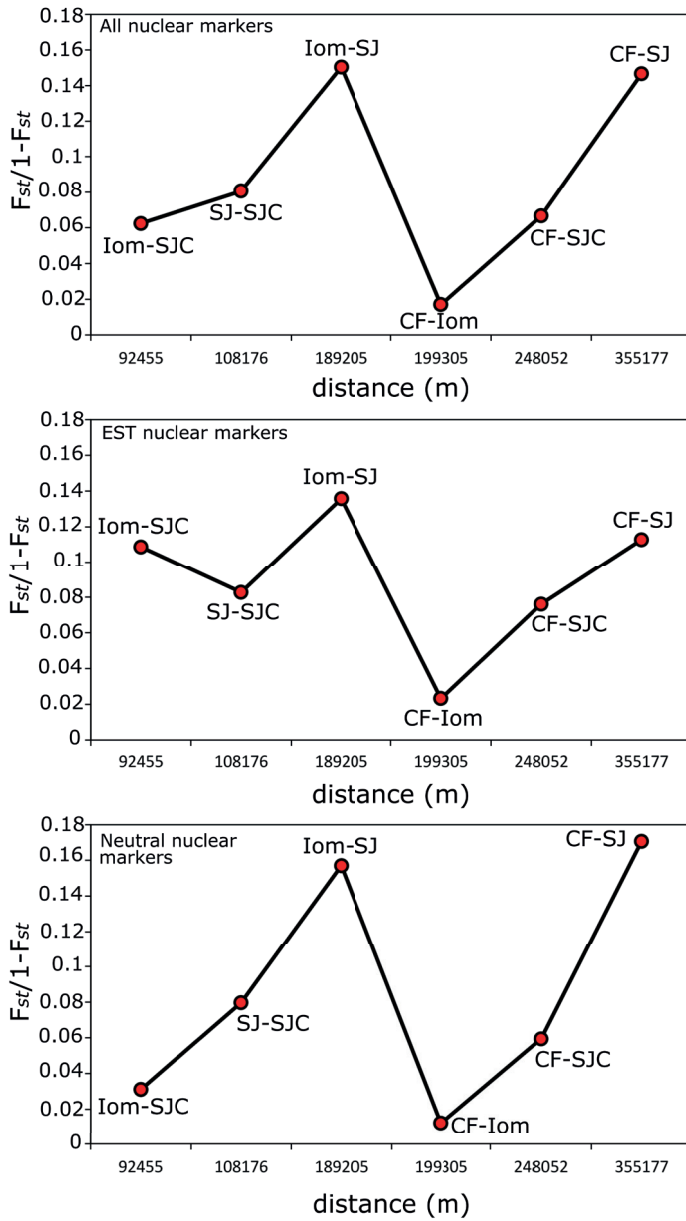


Figure 3. Plot of pairwise $F_{ST}/1-F_{ST}$ estimations against the pairwise geographic distance for forest fragments of *C. xanthocarpa*, based on nuclear microsatellite markers.

Table II. Analysis of molecular variance (AMOVA) estimated considering four categories of SSR markers

	Neutral markers	Gene-linked markers	All nuclear markers	Organellar markers
Molecular variance within forest fragments	93%	94%	93%	81%
Molecular variance among forest fragments (φ_{ST})	7%	6%	7%	19%
p -value of φ_{ST}	0.001	0.001	0.001	0.001

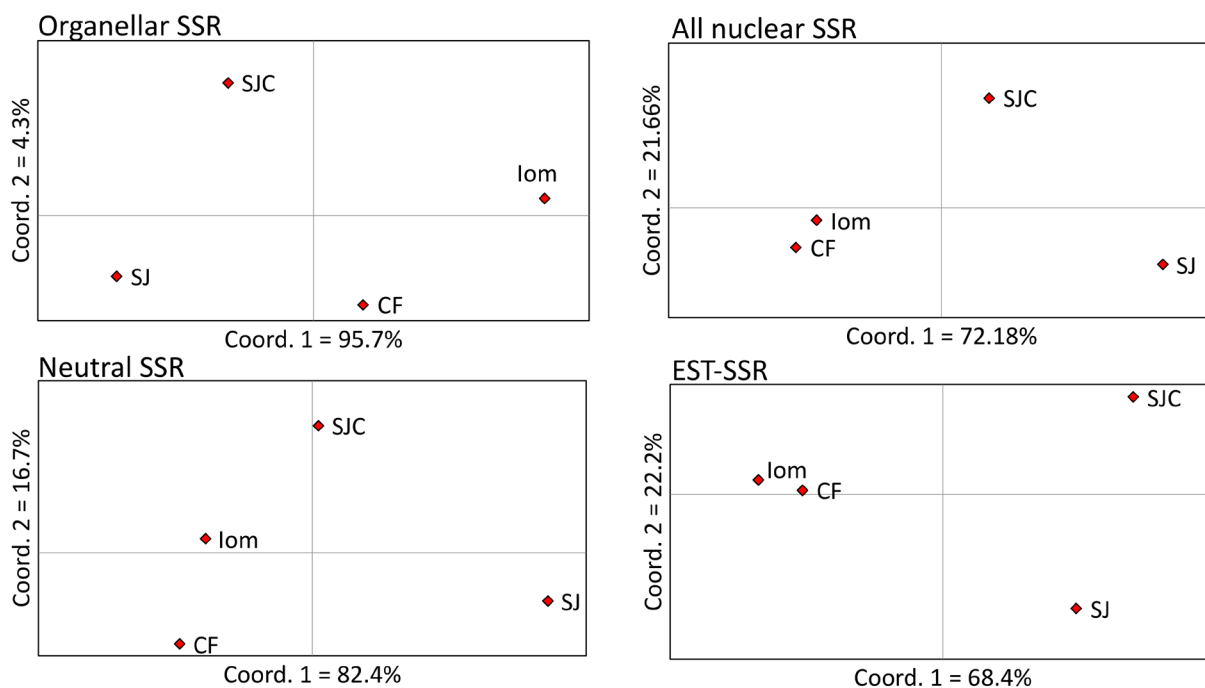


Figure 4. Ordination analysis (PCoA) of the *C. xanthocarpa* studied forest fragments based on organellar microsatellites, all nuclear markers together, neutral markers and gene-linked markers alone.

DISCUSSION

Concerning estimations of genetic diversity, a trend opposite to expected was observed, with the gene-linked SSR markers revealing higher estimations of A , A_e , and H_e in comparison to neutral nuclear microsatellites. Gene-linked markers are directly connected to genes and are expected to be more conserved, while neutral markers are usually hotspots of diversity. In addition, these markers may have a direct influence on population fitness. Thus, they are very useful for the interpretation of the population genetic structure and, together with neutral markers, for taking decisions in conservation issues. Rational conservation decisions can be based on measurements at gene-linked loci of conservation interest without the need for equilibrium assumptions or other complex inferences (Jost et al. 2017).

The gene-linked markers employed in this study are associated with the ADH-3 gene (locus

Cxant69) and with the resistance gene analog RGA2 (locus Cxant76) (Petry et al. 2019). The higher estimations of the number of alleles (A) and the effective number of alleles (A_e) may be related to the numerous functions of the linked-genes. The ADH-3 gene is responsible for coding an alcohol dehydrogenase enzyme, which is related to a wide range of metabolic functions as plant growth, development, adaptation, fruit ripening, and aroma production (Chen et al. 2018). For this locus, the forest fragments SJ and SJC revealed a higher frequency (> 0.5) for allele 289, while CF and IOM presented a higher frequency for allele 330 (Supplementary Material-Table S1). Similarly, the resistance gene analog RGA2 is expected to have several forms (alleles), since it is a hypothetical R -gene responsible for the race-specific resistance in plants. All cloned disease resistance genes in plants belong to several major classes of RGAs (Sekhwal et al. 2015). This SSR locus presented

Table III. Scaled effective size (θ) of each forest fragment, scaled immigration rate (M) and number of migrants per generation (Nm), based on all nuclear SSR markers. Means after three independent runs. The effective sample size (ESS) determines the confidence of the estimations. Pairwise estimates of G_{ST} (fixation) and D (allelic differentiation) are also displayed for each population pair and are independent of the direction of the gene flow.

Effective size parameters				
	θ (percentiles)		ESS	
θ_{CF}	0.09374 (0.085; 0.10)		372947.9	
θ_{Iom}	0.09042 (0.079; 0.10)		317212.9	
θ_{SJ}	0.09216 (0.081; 0.10)		247554.8	
θ_{SJC}	0.09263 (0.081; 0.10)		325348.5	
Migration parameters				
	M (percentiles)	Nm	ESS	G_{ST} / D
$M_{CF \rightarrow Iom}$	478.37 (273.33; 674.00)	43.25	193602.9	0.031 / 0.036
$M_{Iom \rightarrow CF}$	427.75 (0.00; 48.00)	40.10	223356.4	
$M_{CF \rightarrow SJ}$	136.88 (0.00; 80.00)	12.61	199454.7	0.235 / 0.131
$M_{SJ \rightarrow CF}$	33.88 (9.33; 56.67)	3.18	238055.0	
$M_{CF \rightarrow SJC}$	62.95 (30.67; 82.00)	5.83	153475.5	0.123 / 0.121
$M_{SJC \rightarrow CF}$	601.99 (366.67; 905.33)	56.43	205307.4	
$M_{Iom \rightarrow SJ}$	62.84 (38.67; 86.00)	5.79	233460.3	0.227 / 0.123
$M_{SJ \rightarrow Iom}$	61.15 (36.00; 85.33)	5.53	212557.2	
$M_{Iom \rightarrow SJC}$	96.75 (6.00; 95.33)	8.96	208354.5	0.110 / 0.135
$M_{SJC \rightarrow Iom}$	48.72 (12.00 - 75.33)	4.41	202367.7	
$M_{SJC \rightarrow SJ}$	50.49 (24.00; 72.00)	4.65	197266.7	0.139 / 0.078
$M_{SJ \rightarrow SJC}$	247.06 (15.33; 84.00)	22.89	194467.3	

The 2.5% and 97.5% percentiles of the posterior probability are given within parenthesis. Estimations out of the confidence interval (C.I.) are highlighted in bold.

the highest number of alleles ($A = 8$). Analogous to occurred in locus *Cxant76*, some alleles with relatively differentiated frequency are shared between the forest fragments SJ and SJC, as well as between CF and IOM (Table SI).

In addition to such putative plant-parasite factors, climate, and chemical and physical characteristics of the soil are known to shape genetic diversity in forest populations (Baldoni et al. 2020). Thus, the interaction of such abiotic factors with the allelic structure of *C.*

xanthocarpa has to be closely investigated to better understand the evolution of the studied forest fragments.

An important outcome of the present study is the putative differentiated interference of neutral or gene-linked markers in the fine-scale spatial genetic structure (SGS) of forest fragments. In two fragments (CF and IOM), gene-linked markers revealed stronger influence in the slope of the SGS for the closest individuals, suggesting that individuals geographically near to each other

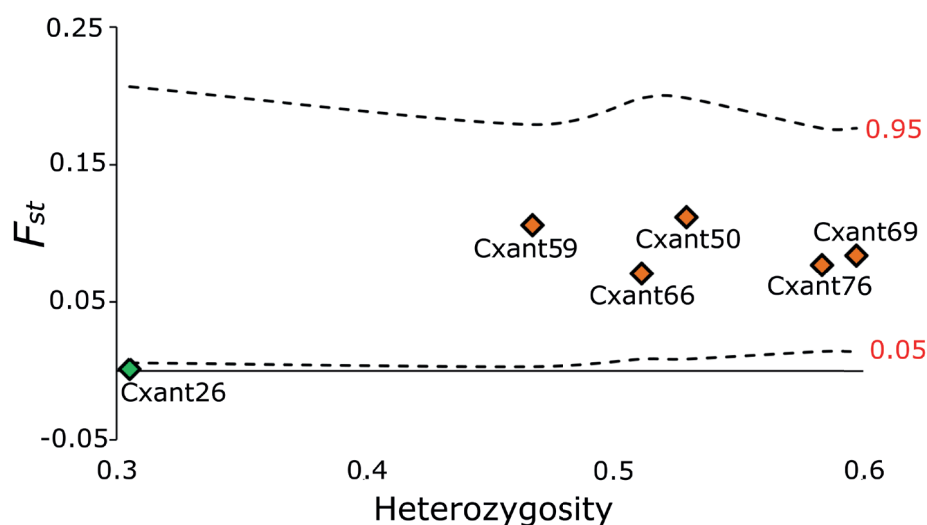


Figure 5. Plot of heterozygosity against F_{ST} estimations for all nuclear microsatellite loci employed in this study. Dashed lines denoted 5 and 95% confidence intervals.

share some expressed characteristics, likely as a response to microenvironmental features. On the other hand, individuals geographically far from each other have the SGS more intensely determined by neutral markers. Otherwise, SJ and SJC forest fragments revealed a stronger influence of neutral markers in both short and large distances, suggesting the absence of such a genetic response to microenvironmental attributes, likely due to the absence of significant differences between microenvironments.

The estimations of population variation, based on the fixation measure G_{ST} and the allelic differentiation measure D , highlight complementary aspects of population structure. In this study, higher estimates of G_{ST} were obtained in comparison to estimates of D , suggesting that the studied populations share the genes present in the gene pool, without high alleles fixation. Complementarily, the estimates of G_{ST} give clues about the historical number of migrants among populations (Jost et al. 2017), interpreting also the closeness to alleles fixation (as higher the G_{ST} estimate, the closer to the fixation are the alleles). These estimates of the nearness to fixation were lower than 0.235 for the pairwise analysis, suggesting the occurrence

of historical gene flow, as demonstrated in the coalescent-based analysis of migration (Table III).

No primary evidence of IBD was observed in this study, with patterns of gene flow largely differing across pairs of forest fragments. For instance, while the pair IOM/SJ revealed about five migrants per generation in both directions, the pair SJC/SJ exhibited 22 migrants from SJ into SJC contrasting with five migrants in the opposite direction. Besides, the geographically closest forest fragments did not reveal a higher number of migrants in comparison to more distant ones.

Based on these results, it seems that the inter-fragments differentiation observed in this study is more an effect of isolation by adaptation (IBA) process, in which effective gene flow is reduced among habitats showing distinctive ecological characteristics (Nagel et al. 2015). However, additional factors may determine the occurrence and the intensity of gene flow among and within forest fragments. For instance, the main pollinators of *Campomanesia* are bees (Almeida et al. 2000, Cordeiro et al. 2017, Nucci & Alves-Junior 2015), that present a limited dispersion area (mean pollen dispersal shorter

than 400 m in the neotropical forests; Braga & Collevatti 2011), smaller than the distance separating the studied forest fragments. Such limited dispersion, therefore, characterizes a pattern of IBD. Thus, both IBA and IBD may be occurring among these forest fragments and should be evaluated in further studies, to detect the most important evolutionary forces shaping the genetic structure of *C. xanthocarpa* in this region. Moreover, the dissimilarity observed in the number of migrants (ranging from 3.18 to 56.43) suggests the existence of geographic barriers to migration. The region where this study was performed is formed by hills and valleys, that may act as barriers for seed and pollen dispersers. The absence of significant geographic barriers due to low distortion of the terrain and large areas with grassland or croplands was the main explanation for the similar number of migrants estimated for 20 pairs of *Luehea divaricata* populations growing in the Brazilian Pampa (Nagel et al. 2015).

Concerning the organellar markers, the featured patterns of genetic diversity and differentiation follow the expected one, with a lower number of alleles and higher inter-fragments differentiation in comparison to nuclear markers. In comparison to the nuclear genome, mitochondrial and plastid genomes have much slower mutation rates in land plants (Smith 2015), resulting in a lower number of alleles. The estimations of genetic differentiation among forest fragments are, in turn, within the expected values for species with a biparental inheritance of the chloroplast ($G_{ST} = 0.18$; Pettit et al. 2005), supporting our results ($\varphi_{ST} = 0.19$); Table III) since we used plastid (maternal inheritance) and mitochondrial (biparental inheritance) markers together. On the other hand, nuclear markers revealed estimations of differentiation among forest fragments ($\varphi_{ST} = 0.07$); Table III) and genetic diversity ($H_e = 0.41-0.50$; Table I)

much lower than reported for plant species with similar life-history traits (F_{ST} ranging from 0.19 to 0.26, $H_e = 0.61 \pm 0.21$; Nybom 2004).

The present study also highlights the importance of identifying the genomic origin of the molecular markers employed in genetic studies. Taking this information into consideration will support researchers to better understand the cause of inter- and intra-fragments genetic structure. This understanding, in turn, is crucial for planning strategies for the conservation and management of forest genetic resources. The forest fragments of *C. xanthocarpa* investigated here demand unambiguous conservation strategies. The existence of a pattern of IBA implies the need for maintenance of the current remnants to assure the conservation of the private alleles, which are essential for forest fragments' survival and also for breeding programs. Moreover, as most of the genetic diversity is found within forest fragments, programs of seed collection or genetic rescue should prioritize a larger number of plants within each fragment, to increase the diversity sampled.

Overall, our study corroborates the "paradox of forest fragmentation" (Kramer et al. 2008) within forest fragments. It is predicted that pollination neighborhoods of small-insect-pollinated woody plants seem to decay as the density declines to provide, therefore, less diverse pollen and proportionally more pollen from close relatives (Breed et al. 2015). A central argument for the paradox of forest fragmentation genetics is that average pollen flow distances may locally increase in fragmented animal-pollinated woody plant populations, genetically buffering these populations (Kramer et al. 2008). Moreover, the existence of overlapping generations of long-lived trees on single sites works towards retarding the loss of genetic diversity (Lowe et al. 2015).

On the other hand, genetic signatures of fragmentation likely require several generations to appear and can take hundreds of years in long-lived tree species (Kramer et al. 2008). Thus, we may continue “just looking in the wrong place” (Lowe et al. 2015), since we only sampled adult trees which represent the pre-fragmentation genetic bank of this area.

By using molecular markers with expected divergent models of inheritance and rate of evolution; the present study sheds light on basal aspects of evolution and ecology of forest fragments of *C. xanthocarpa* growing in the subtropical region of the Atlantic Forest, in southern Brazil. The fine-scale spatial genetic structure revealed different patterns in short and large distance classes, with the distinct influence of gene-linked and neutral markers in driving the genetic structure in each distance class. The presence of an isolation-by-adaptation pattern implies the need for maintenance of the current remnants to assure the conservation of the private alleles. Finally, as the genetic diversity is found predominantly within forest fragments, programs of seed collection and/or genetic rescue should prioritize a larger number of individuals within each fragment, to increase the sampled diversity.

Acknowledgments

The authors would like to thank Conselho Nacional de Desenvolvimento Científico e Tecnológico (CNPq/Brazil) for the financial support (Proc. 307144/2013-5) and scholarships and grants awarded to VSP, VMS (Proc. 152143/2007-6 and 113617/2018-6) and RON. The authors would also like to thank to Coordenação de Aperfeiçoamento de Pessoal de Nível Superior (CAPES/Brazil - Finance Code 001), for scholarships awarded to LOM and GHFK.

REFERENCES

- ALMEIDA MJOF, NAVES RV & XIMENES PA. 2000. Influência das abelhas (*Apis mellifera*) na polinização da gabioba (*Campomanesia* spp.). *Pesq Agropec Trop* 30: 25-28.
- AMARAL SC, BARBIERI SF, RUTHES AC, BARK JM, WINNISCHOFER SMB & SILVEIRA JLM. 2019. Cytotoxic effect of crude and purified pectins from *Campomanesia xanthocarpa* Berg. on human glioblastoma cells. *Carbohydr Polym* 224: 115140.
- AULER NMF, REIS MS, GUERRA MP & NODARI RO. 2002. The genetics and conservation of *Araucaria angustifolia*: I. Genetic structure and diversity of natural populations by means of non-adaptive variation in the state of Santa Catarina, Brazil. *Genet Mol Biol* 25: 329-338.
- BALDONI AB ET AL. 2020. Genetic diversity of Brazil nut tree (*Bertholletia excelsa* Bonpl.) in southern Brazilian Amazon. *For Ecol Manag* 458: 117795. <https://doi.org/10.1016/j.foreco.2019.117795>.
- BEAUMONT MA & NICHOLS RA. 1996. Evaluating loci for use in the genetic analysis of populations structure. *Proc R Soc Lond B* 263: 1619-1626.
- BEERLI P. 2016. Migrate: documentation and program, part of LAMARC. Version 2.0. <http://evolution.ge.washington.edu/lamarc.html>.
- BEERLI P & FELSENSTEIN J. 1999. Maximum-likelihood estimation of migration rates and effective population numbers in two populations using a coalescent approach. *Genetics* 152: 763-773.
- BRAGA AC & COLLEVATTI RG. 2011. Temporal variation in pollen dispersal and breeding structure in a bee-pollinated Neotropical tree. *Heredity* 106: 911-919.
- BREED MF, OTTEWELL KM, GARDNER MG, MARKLUND MHK, DORMONTT EE & LOWE AJ. 2015. Mating patterns and pollinator mobility are critical traits in forest fragmentation genetics. *Heredity* 115: 108-114.
- BROCARD CR, PEDROSA F & GALETTI M. 2018. Forest fragmentation and selective logging affect the seed survival and recruitment of a relictual conifer. *For Ecol Manag* 408: 87-93.
- CARDOZO CML, INADA AC, MARCELINO G, FIGUEIREDO PS, ARAKAKI DG, HIANE PA, CARDOSO CAL, GUIMARÃES RCA & FREITAS KC. 2018. Therapeutic potential of Brazilian Cerrado *Campomanesia* species on metabolic dysfunctions. *Molecules* 23: E2336. doi:10.3390/molecules23092336.
- CATELAN TBS, GAIOLA L, DUARTE BF & CARDOSO CAL. 2019. Evaluation of the in vitro photoprotective potential of ethanolic extracts of four species of the genus

- Campomanesia*. J Photochem Photobiol B Biol 197: 111500.
- CHEN L, WANG Z, CHEN R, HE H, MA J & ZHANG D. 2018. Gene cloning and gene expression characteristics of alcohol dehydrogenase in *Osmanthus Fragrans* var. *semperflorens*. Emir J Food Agricul 30: 820-827.
- CORDEIRO GD, PINHEIRO M, DÖTTERL S & ALVES-DOS-SANTOS I. 2017. Pollination of *Campomanesia phaea* (Myrtaceae) by night-active bees: a new nocturnal pollination system mediated by floral scent. Plant Biol 19: 132-139.
- DE PAULO FARIAS D, NERI-NUMA IA, ARAÚJO FF & PASTORE GM. 2020. A critical review of some fruit trees from the Myrtaceae family as promising sources for food applications with functional claims. Food Chem 306: 125630.
- DOYLE JJ & DOYLE JL. 1990. Isolation of plant DNA from fresh tissue. Focus 1: 13-15.
- EXCOFFIER L, LAVAL G & SCHNEIDER S. 2005. Arlequin ver. 3.0: an integrated software package for population genetics data analysis. Evol Bioinformatics Online: 1: 47-50.
- HADDAD NM ET AL. 2015. Habitat fragmentation and its lasting impact on Earth's ecosystems. Sci Adv 1: e1500052.
- HARDY OJ & VEKEMANS X. 2002. SPAGeDi: a versatile computer program to analyse spatial genetic structure at the individual or population levels. Mol Ecol Notes 2: 618-620.
- JOST L, ARCHER F, FLANAGAN S, GAGGIOTTI O, HOBAN S & LATCH E. 2017. Differentiation measures for conservation genetics. Evol Appl 11: 1139-1148.
- KRAMER AT, ISON JL, ASHLEY MV & HOWE HF. 2008. The Paradox of Forest Fragmentation Genetics. Conserv Biol 22: 878-885.
- LAUTERJUNG MB, MONTAGNA T, BERNARDI AP, SILVA JZ, COSTA NCF, STEINER F, MANTOVANI A & REIS MS. 2019. Temporal changes in population genetics of six threatened Brazilian plant species in a fragmented landscape. For Ecol Manag 435: 144-150.
- LEGRAND CD & KLEIN RM. 1977. Mirtáceas. In: Reitz R (Ed) Flora Ilustrada Catarinense. Herbário Barbosa Rodrigues, Itajaí.
- LEMONS RPM, MATIELO CBDO, BEISE DC, ROSA VG, SARZI DS, ROESCH LFW & STEFENON VM. 2018. Characterization of ptSSR, nSSR and EST-SSR markers for understanding invasion histories and genetic diversity of *Schinus molle* L. Biology 7: 43.
- LISBÔA GN, KINUPP VF & DE BARROS IBI. 2011. *Campomanesia xanthocarpa* (GUABIROBA). In: Coradin L, Siminski A and Reis A (Eds). Espécies nativas da flora brasileira de valor econômico atual ou potencial: plantas para o futuro: Região Sul. MMA, Brasília, p. 159-162.
- LOISELLE BA, SORK VL, NASON J & GRAHAM C. 1995. Spatial genetic structure of a tropical understory shrub, *Psychotria officinalis* (Rubiaceae). Am J Bot 82: 1420-1425.
- LOWE AJ, CAVERS S, BOSHIER D, BREED MF & HOLLINGSWORTH PM. 2015. The resilience of forest fragmentation genetics—no longer a paradox—we were just looking in the wrong place. Heredity 115: 97-99. doi:10.1038/hdy.2015.40.
- MEIRMANS PG & HEDRICK PW. 2011. Assessing population structure: FST and related measures. Mol Ecol Res 11: 5-18.
- NAGEL JC, CECONI DE, POLETTI I & STEFENON VM. 2015. Historical gene flow within and among populations of *Luehea divaricata* in the Brazilian Pampa. Genetica 143: 317-329.
- NUCCI M & ALVES-JUNIOR VV. 2015. Biologia floral e sistema reprodutivo de *Campomanesia adamantium* (Cambess.) O. Berg - Myrtaceae em área de cerrado no sul do Mato Grosso do Sul, Brasil. Interciencia 42: 127-131.
- NYBOM H. 2004. Comparison of different nuclear DNA markers for estimating intraspecific genetic diversity in plants. Mol Ecol 13: 1143-1155.
- PALMEIRIM AF, FIGUEIREDO MSL, GRELLE CEV, CARBONE C & VIEIRA MV. 2019. When does habitat fragmentation matter? A biome-wide analysis of small mammals in the Atlantic Forest. J Biogeog 46: 2811-2825.
- PEAKALL R & SMOUSE R. 2012. GenALEX 6.5: Genetic analysis in excel. Population genetic software for teaching and research an update. Bioinformatics 28: 2537-2539.
- PEREIRA MC, STEFFENS RS, JABLONSKI A, HERTZ PF, RIOS ADE O, VIZZOTTO M & FLÔRES SH. 2012. Characterization and antioxidante potential of Brazilian fruits from the Myrtaceae family. J Agric Food Chem 60: 3061-3067. doi:10.1021/jf205263f.
- PETRY VS, STEFENON VM, MACHADO LO, KLABUNDE GHF, PEDROSA FO & NODARI RO. 2019. Repetitive genomic elements in *Campomanesia xanthocarpa*: prospection, characterization and cross-amplification of molecular markers. 3 Biotech 9: 423.
- PETTITRJ, DUMINILJ, FINESCHIS, HAMPEA, SALVINI D & VENDRAMIN GG. 2005. Comparative organization of chloroplast, mitochondrial and nuclear diversity in plant populations. Mol Ecol 14: 689-701. doi: 10.1111/j.1365-294X.2004.02410.x
- ROUSSET F. 2008. Genepop'007: A Complete Re-Implementation of the Genepop Software for Windows and Linux. Mol Ecol Resour 8: 103-106.

RUSCHEL AR, MOERSCHBACHER BM & NODARI RO. 2007. The genetic structure of *Sorocea bonplandii* in South Brazilian forest fragments. *Silvae Genet* 56: 51-58.

SALMAZZO GR, VERDAN MH, SILVA F, CICARELLI RM, MOTA JDS, SALVADOR MJ, DE CARVALHO JE & CARDOSO CAL. 2019. Chemical composition and antiproliferative, antioxidant and trypanocidal activities of the fruits from *Campomanesia xanthocarpa* (Mart.) O. Berg (Myrtaceae). *Nat Prod Res* 15: 1-5. doi:10.1080/14786419.2019.1607333.

SANTOS PM, BAILEY LL, RIBEIRO MC, CHIARELLO AG & PAGLIA AP. 2019. Living on the edge: Forest cover threshold effect on endangered maned sloth occurrence in Atlantic Forest. *Biol Conserv* 240: 108264.

SEKHWAL MM, LI P, LAM I, WANG X, CLOUTIER S & YOU FM. 2015. Disease Resistance Gene Analogs (RGAs) in Plants. *Int J Mol Sci* 16: 19248-19290. doi:10.3390/ijms160819248.

SMITH DR. 2015. Mutation Rates in Plastid Genomes: They Are Lower than You Might Think. *Genome Biol Evol* 7: 1227-1234. doi:10.1093/gbe/evv069.

SOUSA JA ET AL. 2019. Anti-hyperlipidemic effects of *Campomanesia xanthocarpa* aqueous extract and its modulation on oxidative stress and genomic instability in Wistar rats. *J Toxicol Environ Health Part A* 82: 1009-1018.

SOUZA-MOREIRA TM, SALVAGNINI LE, SANTOS E, SILVA VY, MOREIRA RR, SALGADO HR & PIETRO RC. 2011. Antidiarrheal activity of *Campomanesia xanthocarpa* fruit. *J Med Food* 14: 528-531. doi:10.1089/jmf.2009.0278.

STEFENON VM, REE JF, PINHEIRO MVM, GOETEN D, STEINER N & GUERRA MP. 2020. Advances and constraints in somatic embryogenesis of *Araucaria angustifolia*, *Acca sellowiana*, and *Bactris gasipaes*. *PCTOC* 143: 241-263. doi:10.1007/s11240-020-01928-w.

VEKEMANS X & HARDY OJ. 2004. New insights from fine-scale spatial genetic structure analyses in plant populations. *Mol Ecol* 13: 921-935.

VIECILI PRN ET AL. 2014. Effects of *Campomanesia xanthocarpa* on inflammatory processes, oxidative stress, endothelial dysfunction and lipid biomarkers in hypercholesterolemic individuals. *Atherosclerosis* 234: 85-92.

SUPPLEMENTARY MATERIAL

Table S1

How to cite

PETRY VS, STEFENON VM, MACHADO LO, DA COSTA NCF, KLABUNDE GHF & NODARI RO. 2021. Patterns of genetic diversity, spatial genetic structure and gene flow in *Campomanesia xanthocarpa*: insights from SSR markers of different genomic origins. *An Acad Bras Cienc* 93: e20210134. DOI 10.1590/0001-3765202120210134.

*Manuscript received on January 28, 2021;
accepted for publication on March 17, 2021*

VANESSA S. PETRY¹

<https://orcid.org/0000-0003-3242-2075>

VALDIR M. STEFENON^{1,2}

<https://orcid.org/0000-0003-1091-700X>

LILIAN O. MACHADO¹

<https://orcid.org/0000-0002-4172-2283>

NEWTON C.F. DA COSTA³

<https://orcid.org/0000-0002-1120-9788>

GUSTAVO H.F. KLABUNDE⁴

<https://orcid.org/0000-0002-0327-0685>

RUBENS O. NODARI¹

<https://orcid.org/0000-0002-8884-2426>

¹Programa de Pós-Graduação em Recursos Genéticos Vegetais, Universidade Federal de Santa Catarina, Departamento de Fitotecnia, Rod. Admar Gonzaga 1346, 88034-000 Florianópolis, SC, Brazil

²Programa de Pós-Graduação em Ciências Biológicas, Universidade Federal do Pampa, Rodovia Osvaldo Aranha, BR 290, Km 423, 97307-020 São Gabriel, RS, Brazil

³Universidade do Estado de Santa Catarina, Centro de Ciências Agrárias, Av. Luiz de Camões, 2090, 88520-000 Lages, SC, Brazil

⁴Empresa de Pesquisa Agropecuária e Extensão Rural de Santa Catarina (EPAGRI), Rod. Antônio Heil, 6800, 88318-112 Itajaí, SC, Brazil

Correspondence to: **Rubens O. Odari**

E-mail: rubens.nodari@ufsc.br

Author contributions

VSP and RON conceived and designed the study; VSP conducted the fieldwork; VSP, LOM, GHFK, and NCF conducted laboratory experiments; VSP, VMS, and LOM analyzed the data; VMS wrote the manuscript, all authors read and approved the final version.

